International Journal of Pharmaceutics 408 (2011) 138–151

Contents lists available at ScienceDirect

International Journal of Pharmaceutics

journal homepage: www.elsevier.com/locate/ijpharm

Pharmaceutical Nanotechnology

Evaluation of a crystalline nanosuspension: Polymorphism, process induced transformation and *in vivo* studies

Puneet Sharma[a,1], Zoran D. Zujovic[b], Graham A. Bowmaker[b], William A. Denny[c], Sanjay Garg[a,*]

[a] School of Pharmacy, The University of Auckland, Private Bag 92019, Auckland, New Zealand
[b] Department of Chemistry, The University of Auckland, Private Bag 92019, Auckland, New Zealand
[c] Auckland Cancer Society Research Centre, The University of Auckland, Private Bag 92019, Auckland, New Zealand

ARTICLE INFO

Article history:
Received 21 August 2010
Received in revised form
20 December 2010
Accepted 17 January 2011
Available online 25 January 2011

Keywords:
High pressure homogenization
Solid state
Nanosuspension
Wet milling
Polymorph
Process induced transformation

ABSTRACT

The aim of this work was to evaluate a crystalline nanosuspension of an investigational anticancer compound, SN 30191. Solid forms of SN 30191 were prepared and characterized by thermal analysis, infrared spectroscopy, ^{13}C CP/MAS SSNMR spectroscopy, SEM and powder XRD. Wet milling was performed using a high pressure homogenizer and process induced transformations were studied as a function of time and pressure using infrared spectroscopy. Dose-toxicity and pharmacokinetics (PK) of the nanocrystal formulation were evaluated in mice after intravenous administration. SN 30191 was found to exist in two polymorphic forms (I and II) and a hydrate with an equilibrium solubility < 0.1 μg/ml (pH 1.3–11.0, 37 °C). Wet milling resulted in solid state transformation as a function of pressure. Form II was found to transform into form I at intermediate pressures. A further increase in pressure resulted in formation of a hydrate. The final nanosuspension consisted of SN 30191 as a hydrate. The dose-toxicity studies revealed higher tolerance (~4 times) for the nanosuspension (10 mg/kg) when compared with a solution formulation (2.5 mg/kg). Compared with solution formulation, the nanosuspension allowed the delivery of a higher dose and rendered possible the performance of PK and tissue distribution studies in animals.

1. Introduction

Nanosuspension can be used as a formulation approach when pH modification, co-solvents, surfactants and cyclodextrins are not sufficient for the solubilization of a compound. Especially for compounds at an early stage in drug discovery, nanosuspensions are useful because co-solvents, surfactants and cyclodextrins, which can *per se* modulate the PK of a compound, are avoided (Li and Zhao, 2007). Although, nanosuspension can also alter the PK of a molecule, depending on the dissolution rate of nanoparticles in the blood, it is an important drug delivery strategy for 'brickdust' compounds, which cannot be delivered using other approaches.

SN 30191 is an anti cancer compound synthesized by the Auckland Cancer Society Research Centre (ACSRC), the University of Auckland, New Zealand. Chemically, SN 30191 is an aniline analogue with a molecular weight of 350 g/mol (Fig. 1). It was synthesized as an inhibitor of phosphatidylinositol 3-kinase (PI3-K). This enzyme is a critical component in a major signal transduction pathway that controls various physiological processes including cell differentiation and proliferation. Its activation and/or overexpression has been linked to a number of human cancers, by disruption of the fine equilibrium between cell division, growth and apoptosis leading to abnormal cell growth and possibly resistance to therapy. Due to these reasons the PI3-K pathway is an attractive target for anticancer drug discovery (Hennessy et al., 2005).

Screening assays and cellular inhibition studies performed in the ACSRC suggested that SN 30191 is a potential anticancer compound. However, it is very poorly water soluble (<0.1 μg/ml at 25 °C in water). Therefore, a nanosuspension formulation of SN 30191 was developed to facilitate its toxicity and pharmacokinetic studies. Wet milling by high pressure homogenization (HPH) technique was used to prepare SN 30191 nanosuspension. In the presence of high energy input during milling, there is a possibility of polymorphic transformations in a drug (Sharma et al., 2009). There are currently no reports about the existence of different solid forms (polymorphs, hydrates or solvates) of SN 30191. Therefore, the first aim was to investigate polymorphism in SN 30191. Solid forms of SN 30191 were prepared by different crystallization techniques and subsequently characterized using differential scanning calorimetry (DSC), thermal gravimetric analysis (TGA), infrared (IR) spectroscopy, ^{13}C CP/MAS (cross polarization magic angle) solid state nuclear magnetic resonance (SSNMR) spectroscopy, scanning electron microscopy (SEM) and powder X ray diffraction (PXRD). The second aim of the study was to prepare and characterize a

* Corresponding author. Tel.: +64 9 373 7599x82836; fax: +64 9 367 7192.
E-mail address: s.garg@auckland.ac.nz (S. Garg).
[1] Present address: School of Pharmacy, University of Connecticut, 69 North Eagleville Road, Storrs, CT 06269, USA.

0378-5173/$ – see front matter © 2011 Elsevier B.V. All rights reserved.
doi:10.1016/j.ijpharm.2011.01.032

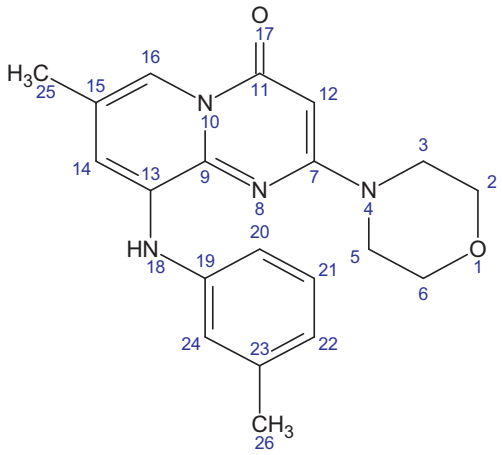

Fig. 1. Structure of SN 30191.

nanosuspension of SN 30191. The formulations were evaluated for particle size, changes in the solid state during and after wet milling, and physical and chemical stability. Dose-toxicity studies of SN 30191 were performed as an i.v. solution and nanosuspension formulation. The highest non-toxic dose selected from the toxicity studies was used in the PK and tissue distribution studies. Throughout this manuscript the term 'HPH' has been used synonymously with 'wet milling'.

2. Materials and methods

2.1. Materials

Solutol® HS 15 (S15) and Cremophor® ELP were received as gift samples from BASF (Germany). Poloxamer 407 (P407) was purchased from Sigma (USA). Acetonitrile and methanol (HPLC grade) were purchased from Ajax Fine Chemicals (Australia). PEG 300 was purchased from Applichem GmbH (Germany). Mannitol, dimethyl sulfoxide (DMSO) and acetic acid glacial (HPLC Grade) were purchased from Scharlau Chemie (Spain). All other reagents, solvents, chemicals and solutions used were of AR grade. Water used in the preparation of the mobile phase, formulations and buffers was obtained by reverse osmosis (MilliQ unit, Millipore, USA) of demineralized water.

2.2. Methods

2.2.1. Preparation of SN 30191 solid forms

Different crystallization techniques were utilized to prepare the solid forms of SN 30191. For each technique, experiments were performed in duplicate.

2.2.1.1. Crystallization by solvent evaporation. SN 30191 was dissolved (0.4–1.0%, w/v, according to the solubility at 60 °C) in 2 ml of the selected solvents with varying polarities (Table 1). The solution was filtered immediately into a 10 ml glass vial and kept at room temperature in order to evaporate the organic solvent. After solvent evaporation, the residue was vacuum dried at 30 °C for 24 h to ensure complete solvent removal from the solid residue.

2.2.1.2. Precipitation in water. SN 30191 (20 mg) was dissolved in a water miscible organic solvent (as specified in Table 1). An accurate volume of this solution was poured into 4 ml of water with constant stirring for 10 min. The resulting dispersion containing the precipitated particles was filtered through a 0.2 μm nylon filter, and the solid mass retained on the surface of the filter was collected and vacuum dried at 30 °C for 24 h for complete solvent removal.

Table 1
Various solvents and preparative conditions used and the corresponding solid forms obtained for SN 30191.

Solvents and conditions	Dielectric constant	Solid forms
Crystallization by solvent evaporation		
Acetone (1.0)[a]	20.5	I[b]
Acetonitrile (0.6)	35.7	I
Tetrahydrofuran (0.8)	7.4	I
Methanol (0.4)	32.6	II[b]
Ethanol (0.4)	24.8	I
Isopropyl alcohol (0.5)	20.2	I
Ethyl acetate (0.7)	6.0	I
Dichloromethane (1.0)	8.9	I
Dioxane (0.8)	2.2	I
Toluene (0.8)	2.4	I
Precipitation in water		
Dimethyl formamide	37.2	H[b]
N-methyl pyrrolidone	32.2	H
Dioxane	2.2	H
Crystallization from acetone		
Rapid cooling	20.5	I
Slow cooling	20.5	I
Slow cooling, seeding with form I	20.5	I
Slow cooling, seeding with form II	20.5	I

[a] Drug concentration (%, w/v) in parenthesis.
[b] I: form I; II: form II; H: hydrate; dielectric constant values for solvents were obtained from reference (Gu et al., 2004).

2.2.1.3. Crystallization from acetone. SN 30191 (1%, w/v) was dissolved in acetone (4 ml) at 60 °C on a water bath. The warm solution was filtered immediately and allowed to cool for 60 min either at −20 °C or at room temperature. In addition, seeds of the solid forms obtained from solvent evaporation were added to the filtrate and kept at room temperature until the acetone was completely evaporated. Following solvent evaporation, the residue was vacuum dried at 30 °C for 24 h to ensure complete dryness.

All the samples obtained from the above mentioned procedures were characterized by DSC, TGA, IR and SSNMR spectroscopy, SEM and PXRD.

2.2.2. Nanosuspension formulation: HPH

HPH was performed using a piston gap high pressure homogenizer, Emulsiflex C-3 (Avestin Inc., Canada) attached to a heat exchanger (Avestin Inc., Canada). The stabilizer solution was prepared by dissolving P407 (1%, w/v) in deionized water, either alone or in combination with 0.5% (w/v) S15.

2.2.2.1. Pre-milling. SN 30191 powder was dispersed at 1% (w/v) in 50 ml stabilizer solution and premilled using an ultra-turrax homogenizer (IKA Werke GmbH and Co., Germany). Precautions were taken to avoid any generation of air bubbles during premilling. After 30 min of pre-milling 25 ml was separated as a pre-milled sample and the rest (25 ml) was used for high pressure homogenization.

2.2.2.2. HPH. The pre-milled suspension (25 ml) was subjected to HPH by applying 10 pre-homogenization cycles at 500 bar followed by 10 cycles at 1000 bar. Finally, homogenization was achieved by applying 20 cycles at 1500 bar followed by 20 cycles at 1750 or 2000 bar. Following this, formulations were collected in 30 ml glass vials. Three formulations were prepared for each stabilizer composition.

2.2.3. Characterization

Different techniques were used for the characterization of the compound. To evaluate the effect of wet milling on solid state, pre-milled samples (obtained after dispersing the drug in the aqueous phase with an ultra-turrax homogenizer) were compared to the milled samples (obtained after HPH). In addition, samples were also taken out at different stages of the process for characterization.

2.2.3.1. Particle size analysis. Particle size analysis of the formulations was performed by laser scattering, using a Mastersizer 2000 (Malvern Instruments, UK) instrument. The measurement range for particle size of this instrument is from 0.02 μm to 2000 μm. For measurement, each formulation was added drop-wise to the sample dispersion unit. The laser obscuration range was always maintained between 10 and 20%. A refractive index value of 1.5 was used to analyze the particle size. The analysis was performed in triplicate for each formulation and the average values of volume distribution were reported. Average particle size was expressed as $d(50)$ (50% of the particle volume below a certain size) and $d(90)$ values (90% of particle volume below a particular size). Span was used to describe polydispersity and calculated as $(d(90) - d(10))/d(50)$.

2.2.3.2. SEM. Morphological evaluation of the SN 30191 solid forms was done using SEM. The samples were placed on carbon specimen holders, coated with platinum in a sputter coater (Polaron SC 7640), and observed using a scanning electron microscope, Philips XL30S FEG (Philips, Eindhoven, Netherlands).

2.2.3.3. IR spectroscopy. The IR spectra of suspension samples were recorded on a Bruker Tensor 37 (Bruker Optik, GmbH, Germany) spectrometer using a MIRacle Micro ATR (attenuated total reflectance) attachment with a diamond crystal. For recording of spectra, a drop of suspension was placed on the diamond crystal and compressed lightly using the pressure clamp. Scanning was performed in the 4000–400 cm^{-1} region with a resolution 4 cm^{-1}, from 64 scans. The spectra reported were obtained by subtracting the spectrum of the pure solution without the drug from that of the nanosuspension. Data were analyzed using OPUS software (Bruker Optik GmbH, Germany) version 6.5. For the characterization of solid forms, powder samples were placed on the crystal surface and were compressed lightly using the pressure clamp. The rest of the procedure was the same as described above.

2.2.3.4. DSC studies. For DSC analysis the pre-milled and milled suspension samples were vacuum filtered through a 0.2 μm nylon filter membrane and the wet precipitates were vacuum dried for 24 h to ensure complete dryness. For DSC studies of solid forms, samples were used as such after crystallization and drying.

DSC was performed using a Q1000 Tzero™ module (TA Instruments, USA). Heat flow and heat capacity calibration of the instrument was done using indium and sapphire, respectively. Powder samples (5–10 mg) were taken in crimped aluminium pans and heated at 10 °C/min (unless stated otherwise) above the T_m of the drugs. Data were analyzed using Universal Analysis software (TA Instruments, USA) version 4.1D. All the measurements were performed in duplicate. T_m is reported as the onset temperature.

2.2.3.5. TGA studies. Samples for TGA were prepared in a similar way as for DSC. TGA was performed on a TGA 50 H thermal analysis instrument (Shimadzu Scientific Instruments, USA) linked to data analysis TA-60WS software (Shimadzu Scientific Instruments, USA). 2.5 mg of samples were heated at 10 °C/min in open aluminium pans under a nitrogen purge up to 200 °C and a TGA trace was recorded. All the measurements were performed in duplicates.

2.2.3.6. PXRD studies. Samples for PXRD were also prepared using the same procedure as DSC studies. PXRD diffractograms were recorded using a Bruker AXS diffractometer (D8 Advance, Bruker AXS Inc., USA) with a Cu line as the source of radiation. Standard runs using a 40 kV voltage, 40 mA current and a scanning rate of 0.02°/min over a 2θ range of 2–40° were used. Results were analyzed using Diffrac^{plus} EVA (Bruker AXS Inc., USA) software.

2.2.3.7. ^{13}C CP/MAS SSNMR spectroscopy. The experiments were carried out using a 7 mm Bruker double tuned probe with zirconia rotors. The proton 90° pulse duration was 4.2 μs. The contact time was 1.5 ms. The recycle delay was 2 s and the spectral-width was 40 kHz. Experiments were carried out with 11,000 scans at ambient temperature using samples enclosed in the rotors. The ^{13}C chemical shift scale is referenced to TMS. Samples were rotated at 7000 ± 1 Hz, and the magic angle was adjusted by maximizing the sidebands of the ^{79}Br signal of a KBr sample.

2.2.3.8. Solubility measurement. Solid forms. Solubility studies were performed for forms I, II and hydrate of SN 30191. Phosphate buffers (0.2 M) were prepared and the pH was adjusted from 1.3 to 11.0 using either phosphoric acid or potassium hydroxide. Approximately 0.2–0.5 mg of forms I, II and hydrate of SN 30191 were added into the eppendorf tubes to which 250 μl of different pH buffers were added ($n = 3$). Tubes were vortexed for 1 min and the pH was measured using a micro electrode attached to a pH meter (Mettler Toledo, Switzerland). Samples were then incubated at 37 °C for 36 h in controlled temperature shaking water bath (SBD 50 Bio Maxi Shake, Heto, Denmark). The samples were centrifuged for 5 min at 10,000 rpm and the precipitate along with the supernatant was collected. The IR spectra of the precipitate were recorded on a Bruker Tensor 37 spectrometer with ATR attachment as described above. Supernatant was filtered through 0.2 μm filter and the pH was measured. The supernatant was directly injected onto the HPLC column without further dilution.

Suspension. SN 30191 solubility was measured in pre-milled and milled suspension samples. 0.5 ml of the sample ($n = 3$) was taken in eppendorf tube and centrifuged at 10,000 rpm for 10 min, filtered through 0.2 μm filter and injected onto the HPLC column.

2.2.3.9. Stability testing. The stability studies were conducted to ensure the formulation quality during the period of the toxicity studies (typically 1–2 weeks). Two formulations were prepared (20 ml batch size) and stored at 4 °C for a period of 2 weeks. At each time point (0 week and at the end of 1 and 2 weeks), formulations were taken out and evaluated for assay, content uniformity, particle size distribution and solid state transformations. For estimation of assay and content uniformity, 50 μl ($n = 5$) of the formulation was dissolved in 5 ml acetonitrile by vortexing for 5 min. 50 μl of this stock was further diluted to 1 ml with acetonitrile and 10 μl was injected onto the HPLC column. The concentrations were determined from the calibration curve, and percentage recovery was calculated and expressed as mean ± SD. To determine the chemical stability at each time point, the percentage area of the SN 30191 peak was compared with the total area of all the peaks in the chromatogram. For characterization of the solid state IR spectroscopy was used.

2.2.4. Dose-toxicity, PK and tissue distribution studies

Male mice (C57 BL/6 strain) weighing 25–30 g were obtained from Vernon Jansen Unit, the University of Auckland, New Zealand. The animals were acclimatized for at least 1–2 weeks before experimentation, fed a standard diet and allowed water *ad libitum*. All animal experimental protocols were evaluated and approved by the Animal Ethics Committee, University of Auckland, New Zealand.

2.2.4.1. Dose-toxicity studies. SN 30191 i.v. solution formulation. SN 30191 is practically insoluble in water but soluble in organic solvents. Therefore, different compositions of DMSO, PEG 300, PBS (pH 7.4) and Cremophor® ELP were screened for solubilization of SN 30191. Based on the results, a final composition of 10% (v/v) DMSO, 40% (v/v) PEG 300, 50% (v/v) PBS and 0.5% (w/v) Cremophor® ELP was selected as the vehicle for the dose-toxicity studies of SN 30191.

SN 30191 i.v. nanosuspension formulation. The nanosuspension formulation was prepared using the same methodology as described earlier and the final formulation consisted of 1% (w/v) SN 30191, 1% (w/v) P407, 0.5% (w/v) S15 and 4.4% (w/v) mannitol in water. The osmolality of the formulation was adjusted with mannitol to 295.0 ± 3.2 mOsm/kg and the pH of the formulation was 5.6 ± 0.7.

SN 30191 solution (2.5 and 5 mg/kg) or nanosuspension (2.5, 5, 10, 15 and 20 mg/kg) were administered via the tail vein with a 1 ml Tuberculin syringe (Terumo Syringe, Philippines) fitted with a 26 gauge needle. Two mice were used for each dose and housed separately. Animals were injected with a pre-determined dose using 5 ml/kg as the maximum volume to be injected in a 20 g mouse (Diehl et al., 2001). Control mice (two for each dose) were injected with the appropriate vehicle without the drug. Following the injection, the animals were observed immediately and twice daily thereafter for a period of 14 days. Clinical signs of toxicity such as decreased physical activity, ruffled fur, hunched posture and loss or gain in the body weight were recorded.

2.2.4.2. PK and tissue distribution studies. SN 30191 formulation and administration. Nanosuspension formulations were prepared using the same methodology as described earlier. The highest non-toxic dose (10 mg/kg) selected from the dose-toxicity studies was used for PK and tissue distribution studies. Both, the nanosuspension and control were administered via the tail vein (5 ml/kg) with a 1 ml Tuberculin syringe (Terumo Syringe, Philippines) fitted with a 26 gauge needle. At pre-determined time points (0, 5, 15, 30, 60 and 90 min) three mice were anaesthetized with isoflurane. Blood was collected from retro-orbital sinus into eppendorf tubes containing 7.5% sodium ethylenediamine tetraacetate solution, and centrifuged at 4500 rpm for 15 min for the isolation of the plasma.

The mice were then euthanized by cervical dislocation, and the liver, kidney, heart, and lungs were collected, washed, weighed and homogenized (Ultra-Turrax Homogenizer (IKS T10), IKA Werke GmbH & Co., Germany) in 1 ml of PBS (pH 7.4). After collection, both plasma and tissue samples were stored at −20 °C until analysis. 5 μl of internal standard (5 μg/ml) was added to each of the plasma and tissue homogenate samples. Protein precipitation of the plasma and tissue homogenate samples was carried out by the addition of 1 ml of ice cold acetonitrile. After 1 min vortexing using a VX100 Labnet vortex mixer (Labnet Int., NJ, US), the samples were kept at −20 °C for 30 min. The samples were then centrifuged (Sigma Laborzentrifugen, Germany) at 4500 rpm for 15 min and the clear supernatant was transferred to fresh eppendorf tubes and vacuum dried using a vacuum centrifuge. The dried residue was then reconstituted in 100 μl of mobile phase and 10 μl was injected onto the HPLC column for analysis. A calibration curve was constructed as a linear plot of peak area ratios between SN 30191 and internal standard against the SN 30191 concentrations. A best fit to a straight line was obtained using linear regression analysis.

The lowest standard (i.e., 0.1 μg/ml) on the calibration curve was identified as the lower limit of quantification as the analyte peak was identifiable and reproducible with a precision of less than 20%. A calibration curve was prepared using six calibration standards (0.1–20 μg/ml, 5 μg/ml internal standard). Intra-day and inter-day accuracy and precision were determined by analysis of the 0.25, 2.5 and 10 μg/ml concentrations. The overall precision and accuracy of the method were determined by measuring %RSD and comparing the means of the measured concentrations to their true concentrations, respectively.

2.2.4.3. Analytical method. An Agilent series 1100 LC (Agilent Corporation, Germany) comprising a quaternary pump, an autosampler and photodiode array detector were used with data acquisition by Chemstation® (Agilent Corporation, Germany). Separation of SN 30191 and internal standard (praziquantel) was achieved with a Gemini C_{18} analytical column (250 mm × 4.6 mm, particle size 5 μm) from Phenomenex, USA and a C_{18} precolumn of the same packing (12.5 mm × 4.6 mm). A mobile phase consisting of acetonitrile and 0.2% (v/v) acetic acid solution (65:35) was used at a flow rate of 1 ml/min to elute the compounds. Samples were injected at 20 μl of injection volume and SN 30191and internal standard were analyzed at wavelengths of 268 nm and 215 nm, respectively. The autosampler temperature was maintained at 10 °C and the sample run time was 9 min.

2.2.4.4. Pharmacokinetic analysis. The SN 30191 pharmacokinetic parameters in mice were estimated by non-compartmental analysis (NCA) using WinNonlin software version 5.0 (Pharsight Corporation, USA). The data were fitted to the NCA using a weighed least square algorithm with uniform weighing. The elimination rate constant (λ) was determined as the slope of the terminal phase of log-linear concentration–time curve. The elimination half-life $t_{1/2}$ was calculated as ln(2)/λ. The area under the concentration–time curve (AUC) from time zero to the last quantifiable concentration (C_t) was calculated by the log-linear trapezoidal rule. The AUC extrapolated to infinity was determined from the formula $AUC_{0-\infty} = AUC_{0-t} + C_t/\lambda$. Other parameters, clearance (CL), volume of distribution at steady state (V_{ss}) and mean residence time (MRT) were calculated using the following equations: CL = dose/AUC; V_{ss} = CL × MRT, and MRT = AUMC/AUC where AUMC represents the total area under the first moment of the concentration–time-curve, computed in a similar way to that used for AUC. Statistical analysis was performed by SigmaStat 3.5 using Student's *t*-test or one-way ANOVA and a p value < 0.05 was considered statistically significant.

3. Results and discussion

3.1. Preparation and characterization of solid forms

Two techniques were utilized for the polymorph preparation in the present study, solvent evaporation (using single solvent) and anti-solvent precipitation in water. In addition, the effect of the cooling rate on the polymorph generation was also studied (Table 1).

During the solvent evaporation process, the nature of the solvents employed affect crystallization (Li et al., 1996). Specifically, solvent interaction with the molecular aggregates of the drug present in the supersaturated solution is a determinant of the final crystal form and has been previously reported to affect acetanilide crystallization (Guillory, 1999). In a supersaturated solution, acetanilide exists as chains of hydrogen bonded aggregates, which upon crystallization align along the needle axis and form long needle shaped crystals. Therefore, non-polar solvents that do not disrupt the hydrogen bonding in the acetanilide aggregates result in the formation of needle shaped crystals. On the other hand, solvents that are proton donors or acceptors (such as acetone) compete with the amide molecules in acetanilide for hydrogen bonding sites and inhibit the formation of hydrogen bonded aggregates, resulting in the formation of rod shaped crystals.

Crystallization of SN 30191 was performed using eight solvents with varying polarities. As shown earlier in Table 1, crystallization from all the solvents resulted in form I suggesting that the polarity

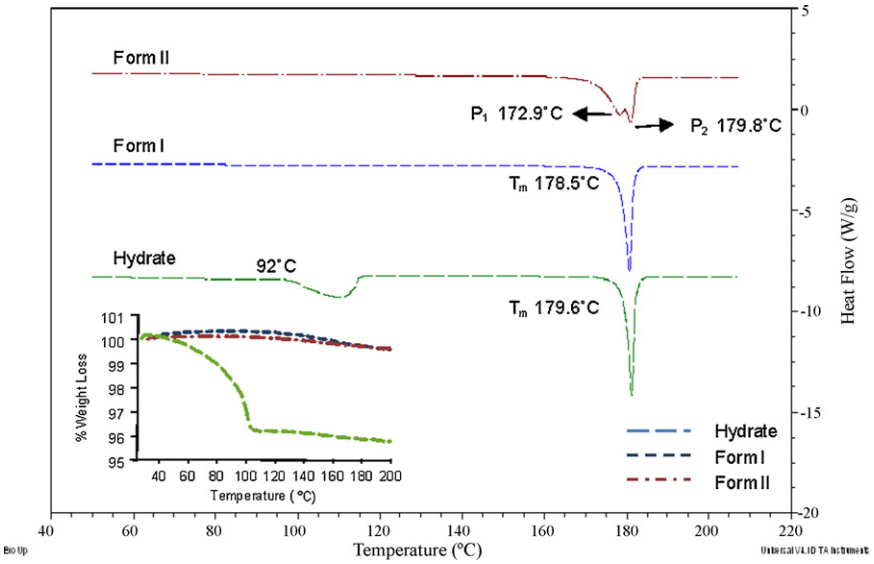

Fig. 2. DSC thermograms and TGA (inset) traces of three solid forms of SN 30191; forms I, II and hydrate. DSC: form II showed concurrent transitions (P_1 and P_2). Form I showed single melting peak with T_m as 178.5 °C. Hydrate showed two endothermic transitions at 92 °C and 179.6 °C. TGA: forms I and II did not show any weight loss up to the melting point. Hydrate showed 3.9% weight loss up to 110 °C and no further weight loss up to the melting point.

of the solvent had no effect on the crystallization of SN 30191. Form II was crystallized from methanol and anti-solvent precipitation resulted in the formation of a hydrate. These three solid forms (I, II and hydrate) were characterized using the different techniques described below. The results obtained for duplicate experiments were consistent in all the cases.

3.2. Characterization of solid forms

The DSC thermogram (Fig. 2) of form I showed T_m at 178.5 °C with an enthalpy of fusion (ΔH_m) of 89.9 J/g (Table 2) whereas form II showed two endothermic peaks (P_1) at 172.9 °C (T_{max} = 178.2 °C) and (P_2) at 179.8 °C (T_{max} = 181.1 °C). For both the solid forms, TGA (inset in Fig. 2) showed no weight loss up to the T_m, indicating an absence of any solvated or hydrated form. The DSC study of form II showed that upon heating it undergoes a concurrent transition at 172.9 °C (P_1) with simultaneous re-crystallization of a new crystalline form (form I). This was followed by the melting of the new form (form I) at 179.8 °C. Due to the concurrent transitions it was difficult to determine the ΔH_m of the lower melting form II and establish thermodynamic stability. To separate the two transitions in form II, high heating rates were utilized, however, increasing the heating rate at more than 20 °C/min resulted in an unstable baseline. Therefore, a maximum heating rate of 20 °C/min was used. As shown in Fig. 3, as compared with lower heating rate, increasing the heating rate to 20 °C/min resulted in the appearance of a better melting peak of form II compared to lower heating rates. However, a clearly separate endothermic peak, which is required for peak integration and calculation of enthalpy, could not be obtained.

Table 2
Thermodynamic parameters derived from DSC of SN 30191 solid forms.

	T_m (°C)	T_{max} (°C)	ΔH_m (J/g)
Form I	178.5	180.6	89.9
Form II	P_1 = 172.9 P_2 = 179.8	178.2 181.1	NA
Hydrate	179.6	181.2	87.4

T_m: melting temperature, T_{max}: peak maximum temperature, ΔH_m: enthalpy of melting. NA: not applicable due to the occurrence of concurrent transition.

Anti-solvent crystallization of SN 30191 resulted in the formation of a different solid form. The DSC thermogram showed two endothermic peaks at approximately 92 °C and 179 °C as onset temperatures and TGA trace indicated a weight loss of 3.9% up to 110 °C (Fig. 2). As the temperature range for this weight loss was close to the boiling point of water, the form obtained following anti-solvent crystallization appeared to have a molecular interaction with water, resulting in the formation of a hydrate. As the T_m for this form at 179 °C is similar to the T_m of form I, it appears that this solid form is a hydrate of form I.

IR spectroscopy was performed to confirm the results obtained from thermal analysis. Each SN 30191 solid form showed a characteristic IR spectrum (Fig. 4). Finger print regions of the three forms showed differences in the bands. As expected, the spectra were dominated by the bands from the pyrido-pyrimidine and meta substituted benzene ring (in the 1600–1500 cm^{-1} region). The hydrate showed two broad bands in the 3400–3500 cm^{-1} region, corresponding to the presence of a free and bonded–OH group. The position of the amide I band (C=O stretching mode in mesomeric effect with N at position 1) was observed at 1672 cm^{-1} in form I and shifted to 1661 cm^{-1} in hydrate. However, the band at 1116 cm^{-1}, due to C–O–C anti-symmetric stretch, remained unchanged in the three solid forms.

Further evidence for the different solid state structures was provided by PXRD patterns, which were different for each solid form (Fig. 5). PXRD peaks were intense and sharp for form I compared to form II, indicating that form II probably has a more disordered structure. Moreover, at high 2θ angles (20–25°), form I peaks were more intense than those for form II, indicating a high degree of crystallinity for form I. The PXRD pattern of the hydrate was different from those of forms I and II. This showed that all the three solid forms have different molecular arrangements in their crystal structure. This was also observed in the SEM micrographs of the three solid forms (Fig. 5). Form I comprised irregular shaped crystals with a non-uniform surface, whereas form II crystals showed a fibrous appearance. The hydrate showed the presence of a mix of thin needle shaped crystals and fibers. The ^{13}C CP/MAS NMR spectra of the two polymorphic forms are shown in Fig. 6. Peak assignments were made by comparison with the chemical shifts obtained from solution NMR (Table 3). Significant differences were obtained in the chemical shifts of the two forms and multiple peaks were observed

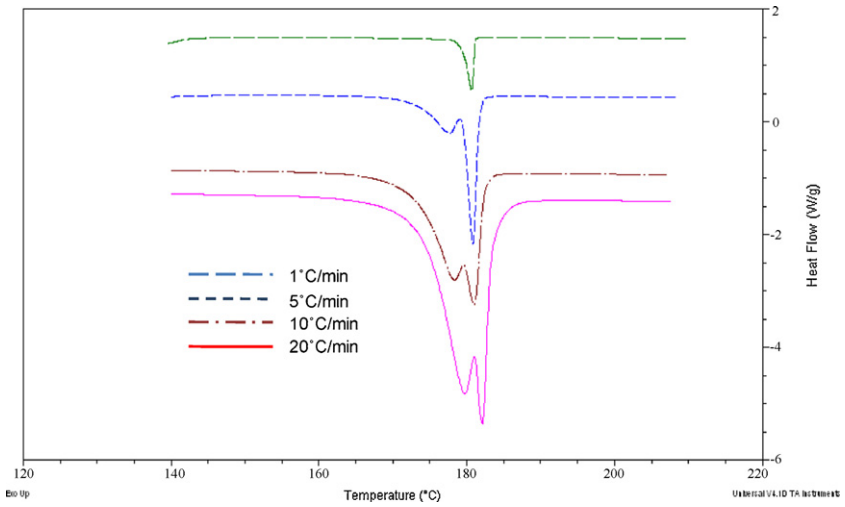

Fig. 3. DSC thermograms of form II of SN 30191 at different heating rates.

for several carbons (e.g. C7, C11, C26, C25, C14, C16). Compared with form 1, peak positions and intensities were different for form 2. These results further supported the presence of two solid forms of SN 30191.

Results of the solubility studies showed that all the three solid forms are poorly soluble in water in the pH range of 1.3–11.0 at 37 °C. This also indicates that the compound is non-ionized over the pH range 1.3–11.0 as ionizable compounds are expected to show higher solubility. SN 30191 peak was not observed in any of the solubility studies samples indicating a solubility of less than 0.1 μg/ml (limit of detection of the assay) for SN 30191. IR spectra obtained for the residue left in the eppendorf tubes did not show any poly-

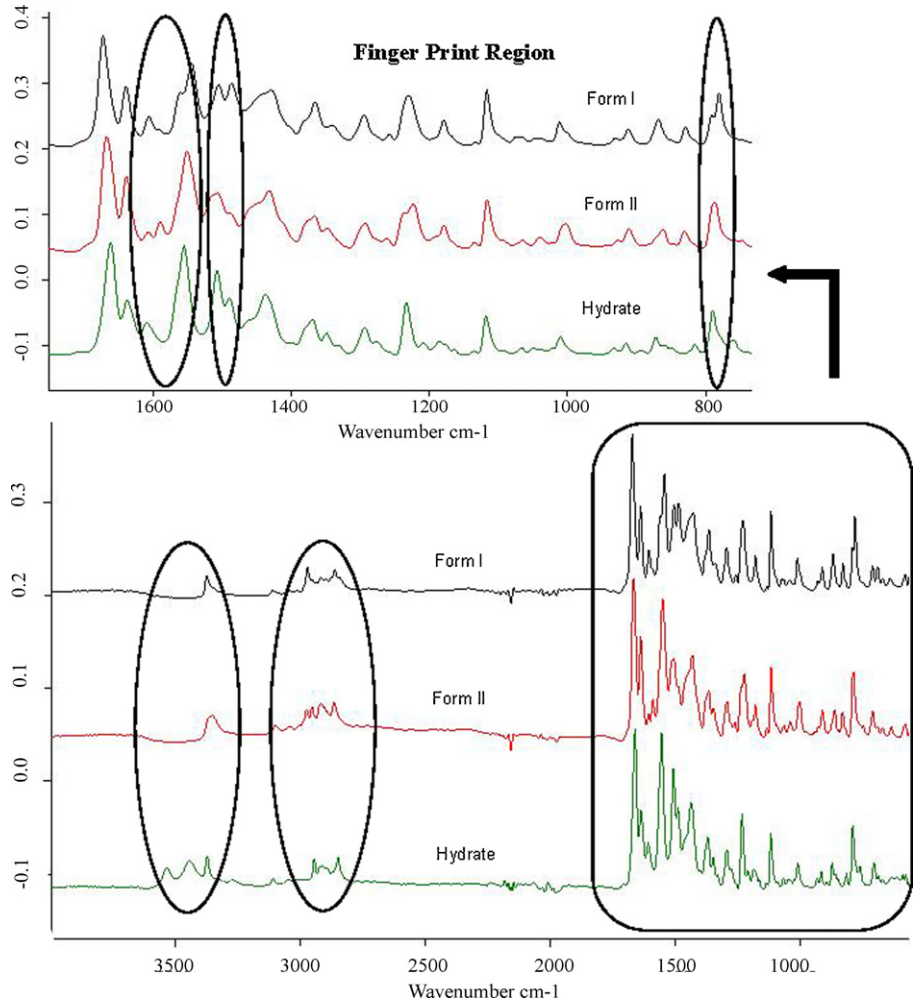

Fig. 4. IR spectra of SN 30191 solid forms; form I, form II and hydrate (top to bottom). The changes observed in the spectra are encircled.

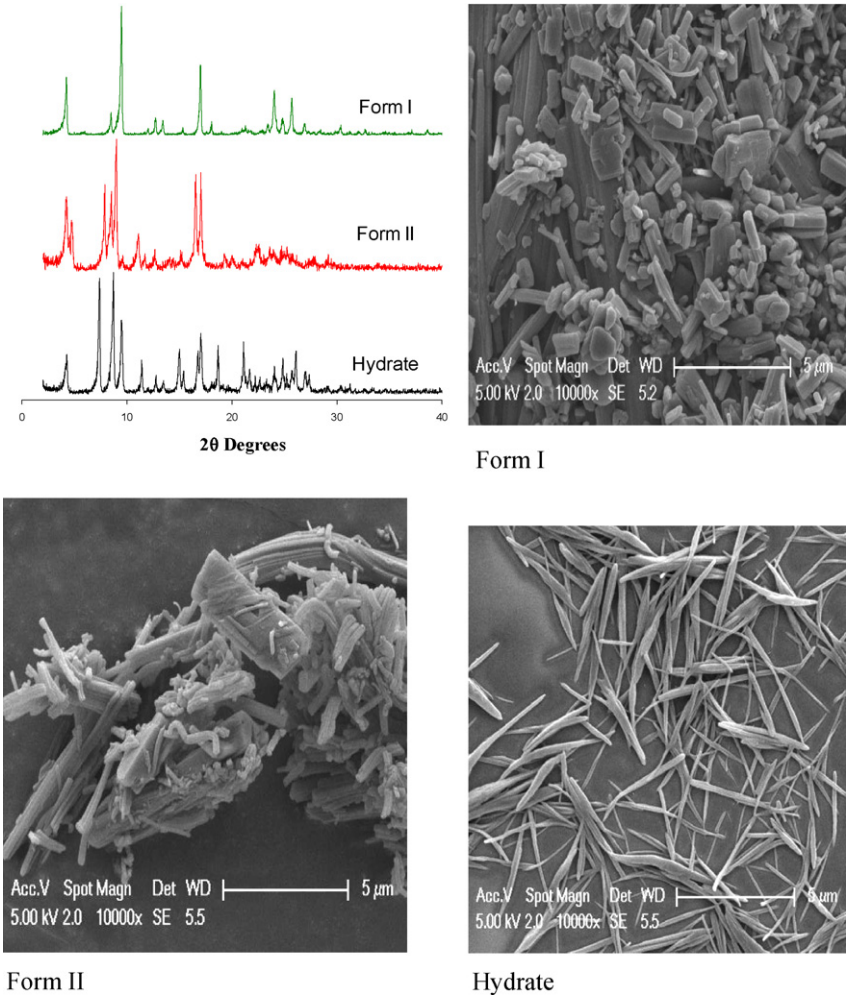

Fig. 5. PXRD and SEM micrographs of SN 30191 solid forms.

morphic transformation during the period of the solubility study, indicating that the poor solubility of the solid forms is not due to a change in the solid state.

Considering SN 30191 as a non-electrolyte, a general solubility equation can be used to predict its solubility (Yang et al., 2002).

$$\log S_u = 0.5 - \log P - 0.01(T_m - 25) \quad (1)$$

Table 3
^{13}C NMR chemical shifts and peak assignments for solid forms of SN 30191.

Assignments	^{13}C chemical shift (ppm)		
	Solution	Form I	Form II
C2	66.5	66.1	65.7
C3	44.7	44.2	42.6
C7	159.8	159.0	158.3
C11	159.1	157.3	157.3
C12	81.9	80.4	79.9
C13	135.7	133.5	136.3
C14	112.6	113.5	113.8
C15	123.0	123.8	–
C16	114.2	114.7	117.6
C19	140.2	140.9	141.9
C20	118.5	–	119.8
C21	129.4	128.4	130.0
C23	139.6	139.3	139.4
C24	122.4	122.8	122.6
C25	18.8	18.8	19.2
C26	21.5	21.5	21.4

where S_u is the molar solubility expressed in mol/l. For calculating solubility using Eq. (1), a melting point of 179 °C was used (as obtained from DSC). A log P value of 4.11 was calculated using Molecular Modeling Pro software (Chemistry Software Ltd., UK). This software calculates log P based on Moriguchi's method (Moriguchi et al., 1992). Putting the T_m (melting point) and log P value in Eq. (1), a solubility value of 2.5 μg/ml was obtained. Although, the value calculated using the above equation was 25 times higher than the experimental value, it shows that SN 30191 is a poorly water soluble compound.

It should be noted that the solubility calculation performed using Eq. (1) does not provide the true solubility of SN 30191, but rather it indicates that SN 30191 has poor water solubility and hence supports the experimental results. There are many methodologies reported in the literature for solubility predictions other than Eq. (1) (Delaney, 2005). These methods are based on some assumptions. When any of the assumptions are not valid, there may be a deviation in the experimental and calculated solubility values. For example, calculation of solubility using Eq. (1) is based on four assumptions (Ran et al., 2002)—(i) van't Hoff equation describes the ideal solubility of a compound and Walden's rule describes the melting entropy (generally 56.5 J/K mol), (ii) log P is equal to the ratio of octanol–water solubility ratio, (iii) for complete miscibility, the molar solubility of a solute in octanol is 3.15 and (iv) in the presence of water the melting point of the solute does not change. Any non-compliance with these assumptions would result in a solubility

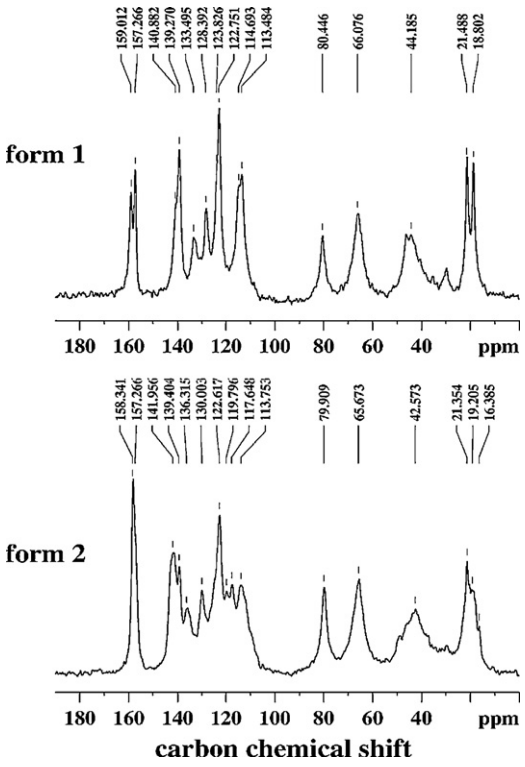

Fig. 6. ^{13}C SSNMR of SN 30191 solid forms.

value different from the true solubility of the compound (Ran et al., 2002).

3.3. Nanosuspension formulation and characterization

1% (w/v) concentration of SN 30191 was used for homogenization. P407 and S15 were selected as the stabilizers. P407 is a copolymer of ethylene oxide (EO) and propylene oxide (PO) blocks that are arranged in a triblock structure EO_x–PO_y–EO_x, represented chemically as $HO[CH_2–CH_2O]_x$ $[CH(CH_3)–CH_2O]_y$ $[CH_2–CH_2O]_xOH$—where y is greater than 14 (Dumortier et al., 2006). It forms micelles at higher concentrations (critical micelle concentration (CMC) of 4% (w/v) in water at 20 °C) (Alexandridis et al., 1994). S15 (macrogol-15 hydroxystearate) is a mixture of about 70% polyglycol mono- and diesters of 12-hydroxystearic acid (lipophilic part) and 30% molecules consisting of polyethylene glycol (hydrophilic part) (Strickley, 2004). S15 forms micelles at low concentrations (0.02%, w/v) (Buszello et al., 2000) and is commonly used as a solubilizing agent in injectables and oral formulations (Strickley, 2004).

To assess the effect of the stabilizer on the physical stability and solubility of SN 30191 nanosuspension, two compositions of stabilizers were employed. Composition A consisted of 1% (w/v) P407 and composition B comprised a mixture of 1% (w/v) P407 and 0.5% (w/v) S15. In composition A, at 1% (w/v) concentration, P407 acts as a non-micelle forming stabilizer and stabilizes the particles through steric effect. However, composition B consisted of a non-micelle forming (P407 at 1%, w/v) as well as a micelle forming stabilizer (S15 at 0.5%, w/v).

Forms I and II of SN 30191 were used for HPH. All the samples were characterized for particle size, solubility and solid state transformation, before and after HPH.

Table 4
Effect of high pressure homogenization and stabilizer on the particle size distribution of SN 30191 forms I and II.

Samples	Span	Size distribution (μm)			% <1 μm
		d(10)	*d*(50)	*d*(90)	
Pre-milled form I	3.44	0.93	4.71	17.12	25
Milled form I + P407	91.31	0.08	0.13	11.95	84
Milled form I + P407+S15	13.38	0.08	0.13	1.82	87
Pre-milled form II	49.51	0.37	1.03	51.37	45
Milled form II + P407	2.5	0.05	0.10	0.30	99
Milled form II + P407+S15	0.9	0.06	0.10	0.15	100

Data shown are the mean values obtained from the particle size analysis of three independently prepared suspensions.
P407: Poloxamer 407, S15: Solutol HS 15; span value ~1 indicate good polydispersity.

3.3.1. Visual observation

Visual observation of the filtered and vacuum dried milled samples did not show any colour change following wet milling and an off-white coloured powder similar to pre-milled sample was observed.

3.3.2. Particle size

The HPH of forms I and II resulted in a significant reduction of the particle size (Fig. 7). 25% of the particles in form I pre-milled sample were below 1 μm (Table 4). Following milling 84% of the particles stabilized with P407 were below 1 μm and 87% with P407 + S15. In the case of form II, 45% of the particles were below 1 μm before milling and more than 99% of the particles were less than 1 μm after milling, using either P407 alone or in combination with S15. The average particle size of the milled forms I and II, with either stabilizer composition, was less than 150 nm.

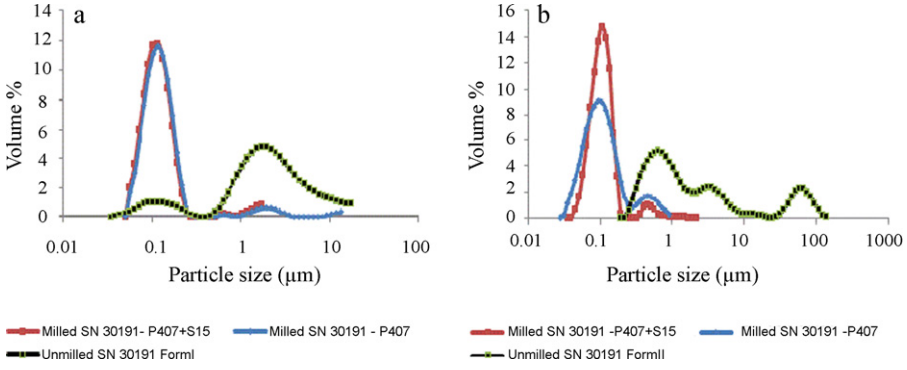

Fig. 7. Particle size distributions of SN 30191 form I (a) and form II (b) before and after high pressure homogenization (P407: Poloxamer 407, S15 – Solutol HS 15). Data shown are the mean values obtained from the particle size analysis of three independently prepared suspensions.

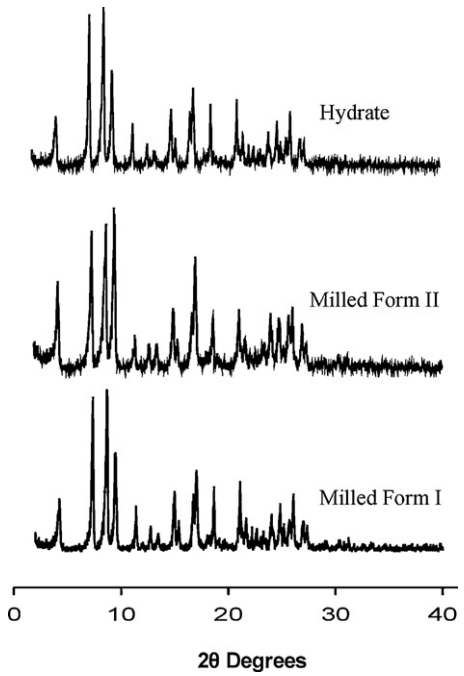

Fig. 8. PXRD patterns of milled SN 30191 (forms I and II with P407 + S15 as stabilizer). PXRD pattern of the hydrate has been included to assist identification of the milled samples.

3.3.3. *Solid state transformation*

HPLC analysis of the samples post-HPH indicated no chemical degradation. The PXRD pattern of the milled samples (both forms I and II) indicated similarities to the hydrate of SN 30191 (Fig. 8). This indicated solid state transformation in forms I and II during HPH.

The DSC thermogram of the milled forms I and II showed three endothermic peaks—P_1, P_2 and P_3 (Figs. 9 and 10). Endothermic peak P_1 was due to P407, P_2 due to the dehydration of the hydrate and P_3 was the melting peak. TGA trace (Fig. 10) also indicated weight loss close to 100 °C, supporting the observation that milling resulted in the formation of the hydrate.

To monitor the solid state transformation during the HPH process, IR spectra of the samples were obtained as a function of homogenization pressure after milling at (a) very low (<500 bar using ultra-turrax); (b) low (500 bar); (c) medium (1000 bar); (d) high (1500 bar) and (e) very high pressures (1750 bar).

During the milling of form II, as the pressure was increased from 500 to 1500 bar an IR spectra corresponding to form I started to appear (Fig. 11). Further increase in pressure to 1750 bar, resulted in the formation of hydrate. However, when homogenization was discontinued after milling up to 1500 bar, hydrate formation was not observed immediately. But after 24 h, the nanosuspension consisted predominantly of hydrate. Form I also showed hydrate formation but only after milling at 1750 bar. However, after milling up to 1500 bar, when stored for 1 week, hydrate formation was not observed in the suspension. The kinetics of hydrate nuclei formation from forms II and I involve considerable energy barrier. The nuclei growth follows from (i) dissolution of metastable solid to form supersaturated solution and (ii) diffusion of 'growing molecular units' to form a stable phase (Zhang et al., 2002). The application of high energy during wet milling of form II up to 1500 bar facilitate the super saturation and formation of stable form I and further application of high energy up to 1750 bar pressure leads to formation of hydrate. When milling is performed using form I, super saturation leading to the formation of hydrate is not produced up to 1500 bar and therefore hydrate formation is not observed.

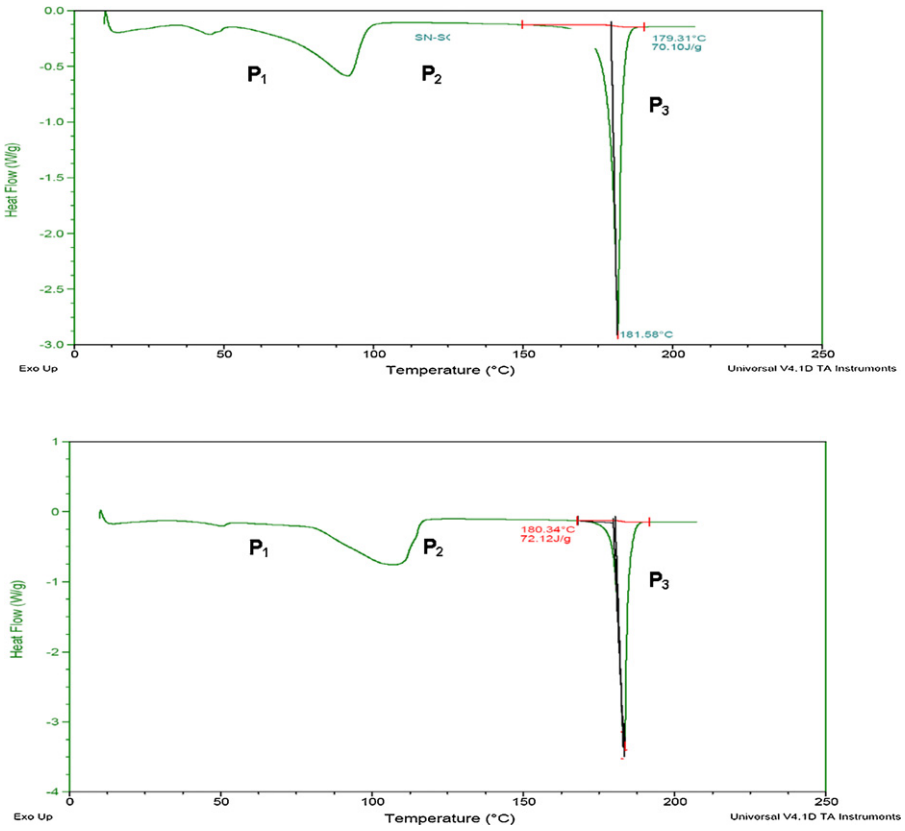

Fig. 9. DSC thermograms of milled form I with P407 (top) and P407 + S15 (bottom) as the stabilizer (P407: Poloxamer 407, S15: Solutol HS 15).

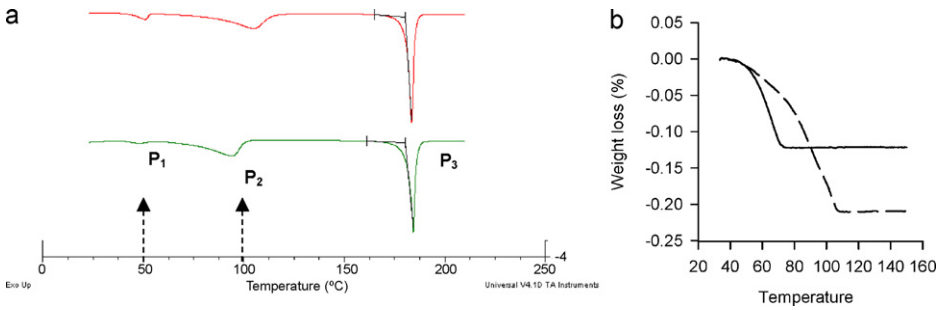

Fig. 10. (a) DSC thermograms of milled form II with P407 (top) and with P407 + S15 (bottom) as the stabilizer. (b) TGA traces of form II with P407 (broken line) and P407 + S15 (solid line) as stabilizers (P407: Poloxamer 407, S15: Solutol HS 15).

IR spectra obtained immediately (0 h) after pre-milling (low pressure homogenization using ultra-turrax) form II showed no change in the spectra (Fig. 12). However, after 24 h, spectral changes were observed, and following 72 h a spectra similar to form I was obtained. Hydrate formation was not observed even after storage for 1 week. This change in the IR spectra was irrespective of the storage temperatures (4 and 25 °C) and stabilizer composition.

Above mentioned results indicate that both forms I and II were stable in dry state at room temperature with a minimal transformation tendency. Low pressure mechanical activation (as applied by ultra-turrax) led to the transformation of form II–I; however, this transformation was relatively slow. When high pressure mechanical activation was applied using a high pressure homogenizer, transformation of form II to form I was rapid. Furthermore, hydrate formation was observed only after mechanical activation of form I at high pressure. The transformation of form II–I and then to hydrate involves a considerable energy barrier which was overcome by application of mechanical energy. In the absence of milling, crystals of forms II and I did not show any transformation tendency when stored for a period of four weeks in stabilizer solution.

Solid state characterization revealed that the nanosuspension formulations consisted of hydrate, irrespective of the solid form initially used for milling. Formation of hydrate may affect other properties such as particle size and solubility. However, particle size analysis of the nanosuspensions showed that with both the stabilizer compositions, the average particle size was less than 150 nm. This indicated that both the stabilizer compositions were effective in preventing the agglomeration of particles. Therefore, the next step was to evaluate the effect of HPH on the solubility of SN 30191 present as hydrate.

3.3.4. *Solubility studies*

Solubility studies of the pre-milled samples (forms I and II) were carried out after 24 h storage following HPH to allow the formation of the hydrate. The solubility of hydrate was <0.1 μg/ml in the presence of P407. In the presence of P407 + S15 (combination) there was an increase in the solubility and mean solubility values were 4.5 μg/ml (initially form I) and 3.9 μg/ml (initially form II), respectively. For the same stabilizer composition, there was no significant difference between the solubility values (Fig. 13).

The presence of S15 at 0.5% (w/v) concentration (more than its CMC) together with P407 increased the solubilization of the dispersed particles through micellization. When used alone, P407 is present as monomers at 1% (w/v) concentration (below its CMC). At this concentration it prevents the agglomeration by steric repulsion, however due to the absence of micellization there was no increase in solubilization.

When compared with pre-milled samples, there was a significant ($p < 0.05$) increase in the solubility of milled samples (Fig. 13). The milled samples showed about a 4-fold increase in solubility in the presence of P407, whereas with the P407 + S15 combination an 8-fold increase was observed compared with pre-milled samples.

Particle size reduction in the nanometer range leads to a significant increase in the surface area of the particles. In addition, there is an increased dissolution pressure and reduced diffusion layer; both these factors lead to an increased solubility of the nanosized

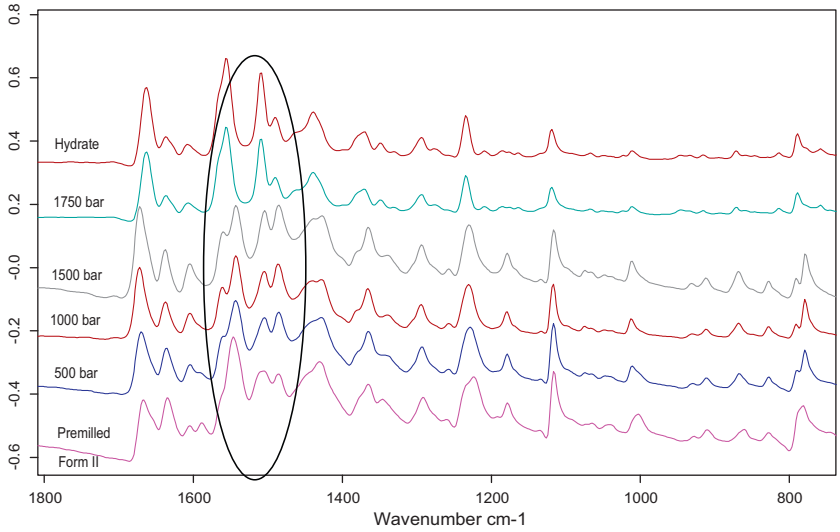

Fig. 11. IR spectroscopy of form II as a function of homogenization pressures (from bottom to top). IR spectrum of the hydrate has been included to assist identification of the samples.

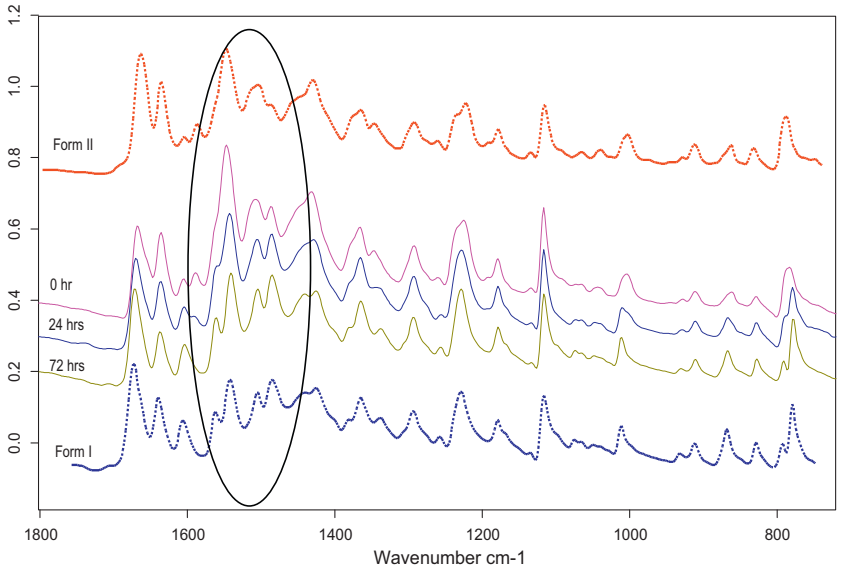

Fig. 12. IR spectroscopy of form II pre-milled suspension sample at different intervals (0, 24 and 72 h, from top to bottom). IR spectra of forms I and II have been included to assist identification of the samples.

drug in water (Galli, 2006; Keck and Muller, 2006). This could be the reason for the increase in the solubility (~4 fold) of milled samples when only P407 was present as the stabilizer. In the presence of the P407 + S15 combination there is an additional solubilization effect due to the presence of S15 micelles (at 0.5%, w/v). The synergistic effect of nanosizing and micellization may be responsible for the greater increase (8-fold) in solubility in the presence of P407 + S15.

Results from the solubility studies show that a combination of P407 + S15 was more efficient in increasing the solubility of SN 30191 than P407 alone. Particle size analysis also showed that for the same stabilizer composition (P407 + S15), the upper end particle size was below 400 nm. It is interesting to note here that although there was a solid state transformation during wet milling, it did not have any significant effect on the particle size distribution.

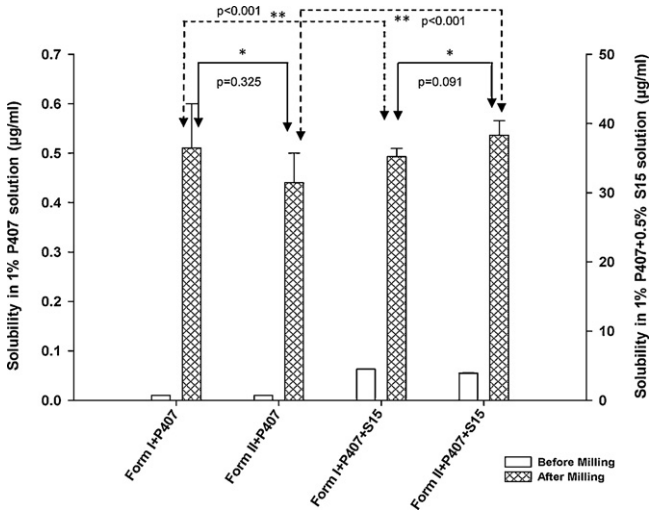

Fig. 13. Solubility of forms I and II of SN 30191 as a function of milling and surfactant composition. After milling there was a significant increase in the solubility of SN 30191. However, between forms I and II, there was no statistically significant ($p > 0.05$) difference (*) in the solubility. Out of the two stabilizer compositions, P407 + S15 combination was more effective ($p < 0.05$) in increasing the solubility of both the forms (P407: Poloxamer 407, S15: Solutol HS 15).

3.4. Stability studies

For the study, two nanosuspensions (20 ml batch size) containing form I (200 mg) were prepared using the procedure described earlier. The stabilizer solution consisted of 1% (w/v) P407 and 0.5% (w/v) S15 in water. Osmolality of the formulation was adjusted to 295.0 ± 2.6 mOsm/kg with mannitol (4.4%, w/v) and the pH of the formulation was 5.8 ± 0.5. Mannitol was dissolved in the stabilizer solution before pre-milling.

The early stage formulations for the animal studies are intended for short term use. Therefore, stability testing was performed for over two weeks. Assay and content uniformity of the formulation was assessed to ensure uniform delivery of doses during *in vivo* studies. Recovery was calculated from the assay results. Average recovery of SN 30191 was approximately 95.5 ± 0.9% (Table 5) for both the formulations. Complete recovery of the drug from the high pressure homogenizer was not possible as some formulation remained inside the pump or homogenization valve, resulting in low recovery values. The content uniformity of the two formulations was good (%RSD < 2.5%) and indicated a uniform dispersion of the particles in the formulation throughout the duration of stability studies. No significant increase in upper end particle size was observed over time indicating the absence of agglomeration.

The chemical stability of SN 30191 was determined by calculating the percentage area of the SN 30191 peak compared with other peaks in the HPLC chromatogram. The placebo sample prepared in the same way as the formulation was also analyzed and area of SN 30191 peak was compared against the placebo peaks for evaluation of degradation. No significant degradation was obtained at any of the time points, indicating a good chemical stability of SN 30191 in the formulation (chromatograms not shown). IR spectra indicated the presence of SN 30191 hydrate in the milled suspension at all the time points.

Despite the solid state transformation during milling, the physical and chemical stability of the formulation was not adversely affected. Therefore, this composition was selected for the dose-toxicity, PK and tissue distribution studies.

3.5. Dose-toxicity studies

SN 30191 is an investigational drug, and thus, there are no reports regarding the maximum tolerated dose (MTD) that can

Table 5
Results of stability studies of SN 30191 nanosuspensions.

Week	0		1		2	
Formulation	A	B	A	B	A	B
Assay 1	195.4	190.2	194.9	190.6	191.2	196.3
Assay 2	191.4	188.4	190.6	190.2	194.9	190.1
Assay 3	190.1	191.1	191.3	188.6	192.4	188.2
Assay 4	192.3	190.0	195.2	186.1	190.2	185.2
Assay 5	193.6	190.2	190.5	189.3	194.2	185.4
Average (mg)	192.6	190.0	192.5	189.0	192.6	189.0
Content uniformity (%RSD)	1.1	0.5	1.2	0.9	1.0	2.4
% recovery	96.3	95.0	96.2	94.5	96.3	94.5
Solid state	Hydrate	Hydrate	Hydrate	Hydrate	Hydrate	Hydrate
Stability (% remaining)	100.0	100.0	99.2	99.5	99.6	99.8
Particle size [$d(90)$] (μm)	1.3	1.2	1.4	1.2	1.3	1.4

Two nanosuspensions A and B were prepared for stability study and at each time point assay was performed on five samples (assay values 1–5). No significant difference (one-way ANOVA) was observed between average assay ($p = 0.97$), % recovery ($p = 0.96$) and particle size ($p = 0.65$) values of the stability samples.

be administered in mice. Therefore, dose-toxicity studies were performed to determine the MTD of SN 30191 as a solution and nanosuspension formulation.

SN 30191 is practically insoluble in water. Therefore, for the preparation of a solution formulation, water soluble organic solvents (DMSO, PEG300) and surfactant (Cremophor® ELP) that are commonly used in the development of early stage formulations were employed (Li and Zhao, 2007). The concentration of each component was within the maximum limit that can be injected safely into animals through an i.v. route without causing any adverse effects (Li and Zhao, 2007).

After i.v. injection of the 2.5 mg/kg SN 30191 solution, one mouse was moribund and hence was euthanized. Moreover, at 5 mg/kg, the mice died within one min of i.v. dosing. However, animals treated with nanosuspension at 2.5, 5 and 10 mg/kg showed no visible signs of toxicity. After administration of nanosuspension at 15 mg/kg dose, one animal was moribund for an initial one min followed by a rapid recovery. In addition, at 20 mg/kg dose, the animals were moribund for a period of 10 h followed by a slow recovery over 24 h. However, no deaths were observed. There was no significant difference in the body weight at any of the doses of nanosuspension formulation for the duration of the study (14 days) compared with the control group. Similar results of an increase in tolerability of a nanosuspension over a solution formulation have been previously reported for itraconazole, where 80 mg/kg of nanosuspension formulations showed no effect on any of the observed parameters compared with a 20 mg/kg dose of a solution formulation (Rabinow et al., 2007).

The MTD determined from the dose-toxicity study of the solution formulation was 2.5 mg/kg. This dose was too low to perform PK studies as the concentration in plasma and tissues would be less than the limit of quantification (0.25 μg/ml) of the HPLC assay. Therefore, PK studies were preformed only for the nanosuspension formulation for which the MTD was 10 mg/kg.

3.6. PK and tissue distribution

The PK and tissue distribution of SN 30191 was determined following i.v. administration of the nanosuspension formulation. The blood concentration–time curve and PK parameters following i.v. administration of SN 30191 nanosuspension (10 mg/kg) are shown in Fig. 14 and Table 6, respectively. The nanoparticles were rapidly cleared from the circulatory system resulting in a short plasma half-life of 0.57 ± 0.15 h and a low plasma AUC value (2.34 ± 0.08 μg ml^{-1} h). Although, PK data for SN 30191 solution formulation is not available for comparison, the CL of nanoparticles from blood seems high (Table 6). In addition, a high value of V_{ss} indicated that the drug was primarily accumulated in tissues.

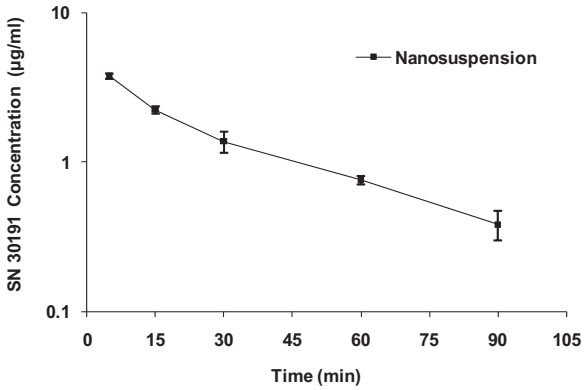

Fig. 14. SN 30191 concentration–time profile in plasma after i.v. administration of nanosuspension at a dose of 10 mg/kg of SN 30191. Each point represents the mean ± SD of $n = 3$ mice.

Following i.v. administration, nanoparticles of a poorly water soluble drug encounter a sink environment in the circulatory system. The following *in vivo* scenarios have been suggested (Wong et al., 2008) regarding the fate of the nanoparticles.

If the drug dissolves immediately after injection it may exhibit a profile similar to the solution formulation of the drug. This has been reported for flurbiprofen (solubility < 10 μg/ml), and the nanoparticle formulation showed a similar pharmacokinetic profile and tissue distribution characteristics to that of the solution formulation (Wong et al., 2008). However, a nanosuspension formulation was preferred over solution as flurbiprofen solution has a higher pH that could be irritating during injection.

If the drug does not dissolve immediately upon injection the nanoparticles will be recognized as foreign matter by the immune system, resulting in opsonization (Wong et al., 2008). Opsonization of nanoparticles depends upon the particle size and surface coating.

A nanoscaled particle (<100 nm) coated with a hydrophilic stabilizer (typically PEG with a molecular weight of 2000) can avoid opsonization and remain circulating in the blood for a longer

Table 6
PK parameters following the i.v. administration of SN 30191 nanosuspension at a dose of 10 mg/kg.

PK parameters	
$AUC_{0-\infty}$ (μg ml^{-1} h)	2.34 ± 0.08
MRT (h)	0.65 ± 0.07
$t_{1/2}$ (h)	0.57 ± 0.15
CL (ml h^{-1} kg^{-1})	4272.05 ± 150.60
V_{ss} (ml/kg)	2766.10 ± 188.32

Values represent the mean ± SD of $n = 3$ mice.

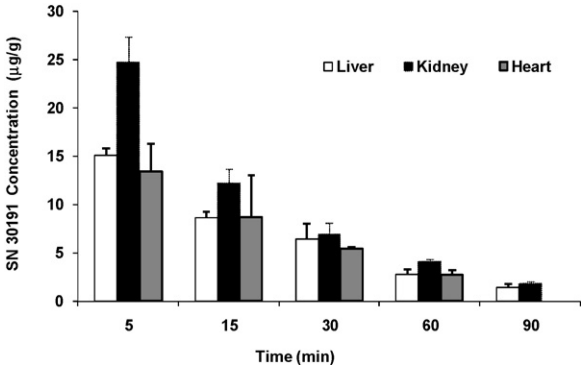

Fig. 15. SN 30191 concentration (normalized to weight) in liver, kidney and heart at different time points following i.v. administration of the nanosuspension at a dose of 10 mg/kg. Each point represents the mean ± SD of $n = 3$ mice.

duration. Long circulating nanoparticles have been reported to selectively accumulate in the tumor through the leaky tumor vasculature by Enhanced Permeability and Retention (EPR) effect (Wong et al., 2008). This results in an enhanced tumor specificity of a drug.

If the particle size or surface coating is not adequate to avoid opsonization of nanoparticles, macrophage uptake may occur. This has been reported for itraconazole (Rabinow et al., 2007) where after injection of nanosuspension (80 mg/kg), the particles were endocytozed in phagolysozome in macrophages of RES organs resulting in a drop in C_{max}. However, due to the continued release of the dissolved drug in the blood after phagocytosis, high AUC was observed. Similar results were reported by Ganta et al. (Ganta et al., 2009) for asulacrine nanosuspension (30 mg/kg) where a drop in C_{max} and higher MRT were observed compared with the solution formulation.

SN 30191 accumulation in the liver, kidney and heart is shown in Fig. 15 and AUC values of the respective tissues are presented in Table 7. A high drug concentration was obtained in the kidney followed by the liver and heart. Furthermore, very low concentrations were observed in the lungs after 5 min (0.41 ± 0.09 μg/ml), following which the concentrations were too low to be determined by the assay.

High concentrations of SN 30191 in kidney, liver and heart indicate a rapid dissolution of SN 30191 nanoparticles in the blood following i.v. administration. The factors that may aid rapid dissolution include the nanometer size (less than 150 nm) of the particles and the micellization effect of the stabilizers. Moreover, SN 30191 is a lipophilic compound (log P 4.11) and after dissolution in the blood it is expected to distribute more in the tissues as compared to the blood (Ritschel and Kearns, 1998). The high V_{ss} observed in the plasma (Table 6) also supported the higher tissue distribution. However, the possibility of macrophage uptake cannot be completely ruled out. Considering a total blood volume in a mouse to be 1.7 ml (85 ml/kg, Li and Zhao, 2007), at a dose of 10 mg/kg, the total amount of drug in the blood which requires solubilization is 0.117 mg. Given that the saturation solubility (and hence the dissolution velocity) of the drug is low (less than 0.1 μg/ml), there will be nanosized particles circulating in the blood immediately after i.v. administration. The particles that did not dissolve instantaneously might have been taken up by the liver macrophages leading to a high concentration in liver.

Table 7
Comparison of tissue AUCs following i.v. administration of the nanosuspension at a dose of 10 mg/kg of SN 30191.

Tissues	$AUC_{0-\infty}$ (μg g^{-1} h)
Liver	9.31 ± 0.91
Kidney	12.96 ± 0.44
Heart	8.35 ± 1.11

Values represent the mean ± SD of $n = 3$ mice.

4. Conclusion

SN 30191 is a poorly water soluble anti-cancer compound. Using two crystallization techniques, solvent evaporation and anti-solvent precipitation, two polymorphs (forms I and II) and a pseudopolymorph (hydrate) were prepared and subsequently characterized by different techniques. The three solid forms showed different crystal habits. The solubility of the solid forms was less than 0.1 μg/ml (pH 1.3–11.0, 37 °C). Nanosuspensions of forms I and II were prepared using HPH. During the process, solid state transformations were observed in forms I and II as a function of pressure. The nanoparticles present in the final nanosuspension were characterized as hydrate. Depending upon the stabilizer composition, the particle size distribution and the solubility of the milled sample varied. In the presence of the P407 + S15 combination, uniform particle size distribution with average particle size less than 150 nm and high solubility was obtained. Despite the solid state transformation during HPH, the nanosuspension formulation was stable for a period of two weeks at 4 °C.

The dose-toxicity studies revealed at least a four times higher tolerability for the nanosuspension (10 mg/kg) when compared with the solution formulation (2.5 mg/kg). PK and tissue distribution studies of nanosuspension indicated that SN 30191 was rapidly cleared from the blood and accumulated in the kidney, liver and heart. It is postulated that the high accumulation of SN 30191 in tissues could be due to rapid dissolution of the nanoparticles in the blood, which facilitated distribution in highly perfused tissues. However, to quantitatively evaluate the benefits of a nanosuspension, in terms of PK and tissue distribution, PK data of solution formulation are required. Compared with solution formulation, the nanosuspension allowed the delivery of a higher dose and made it possible to perform PK and tissue distribution studies in animals. These results demonstrate the advantage of nanosuspension over a solution formulation.

References

Alexandridis, P., Holzwarth, J.F., Hatton, T.A., 1994. Micellization of poly(ethylene oxide)–poly(propylene oxide)–poly(ethylene oxide) triblock copolymers in aqueous solutions: thermodynamics of copolymer association. Macromolecules 27, 2414–2425.

Buszello, K., Harnisch, S., Muller, R.H., Muller, B.W., 2000. The influence of alkali fatty acids on the properties and the stability of parenteral O/W emulsions modified with solutol HS 15. Eur. J. Pharm. Biopharm. 49, 143–149.

Delaney, J.S., 2005. Predicting aqueous solubility from structure. Drug Discov. Today 10, 289–295.

Diehl, K.H., Hull, R., Morton, D., Pfister, R., Rabemampianina, Y., Smith, D., Vidal, J.M., van de Vorstenbosch, C., 2001. A good practice guide to the administration of substances and removal of blood, including routes and volumes. J. Appl. Toxicol. 21, 15–23.

Dumortier, G., Grossiord, J.L., Agnely, F., Chaumeil, J.C., 2006. A review of Poloxamer 407 pharmaceutical and pharmacological characteristics. Pharm. Res. 23, 2709–2728.

Galli, C., 2006. Experimental determination of the diffusion boundary layer width of micron and submicron particles. Int. J. Pharm. 313, 114–122.

Ganta, S., Paxton, J.W., Baguley, B.C., Garg, S., 2009. Formulation and pharmacokinetic evaluation of an asulacrine nanocrystalline suspension for intravenous delivery. Int. J. Pharm. 367, 179–186.

Guillory, J.K., 1999. Generation of polymorphs, hydrates solvates and amorphous solids. In: Brittain, H.G. (Ed.), Polymorphism in Pharmaceutical Solids, vol. 95. Marcel Dekker, Inc., New York, pp. 183–226.

Gu, C.H., Li, H., Gandhi, R.B., Raghavan, K., 2004. Grouping solvents by statistical analysis of solvent property parameters: implication to polymorph screening. Int. J. Pharm. 283 (1–2), 117–125.

Hennessy, B.T., Smith, D.L., Ram, P.T., Lu, Y., Mills, G.B., 2005. Exploiting the PI3K/AKT pathway for cancer drug discovery. Nat. Rev. Drug Discov. 4, 988–1004.

Keck, C.M., Muller, R.H., 2006. Drug nanocrystals of poorly soluble drugs produced by high pressure homogenisation. Eur. J. Pharm. Biopharm. 62, 3–16.

Li, P., Zhao, L., 2007. Developing early formulations: practice and perspective. Int. J. Pharm. 341, 1–19.

Li, R., Mayer, P.T., Trivedi, J.S., Fort, J.J., 1996. Polymorphism and crystallization behavior of Abbott-79175, a second-generation 5-lipoxygenase inhibitor. J. Pharm. Sci. 85, 773–780.
Moriguchi, I., Hirono, S., Liu, Q., Nakagome, I., Matsushita, Y., 1992. Simple method of calculating octanol/water partition coefficient. Chem. Pharm. Bull. 40, 127–130.
Rabinow, B., Kipp, J., Papadopoulos, P., Wong, J., Glosson, J., Gass, J., Sun, C.S., Wielgos, T., White, R., Cook, C., Barker, K., Wood, K., 2007. Itraconazole IV nanosuspension enhances efficacy through altered pharmacokinetics in the rat. Int. J. Pharm. 339, 251–260.
Ran, Y., He, Y., Yang, G., Johnson, J.L.H., Yalkowsky, S.H., 2002. Estimation of aqueous solubility of organic compounds by using the general solubility equation. Chemosphere 48, 487–509.
Ritschel, W.A., Kearns, G.L., 1998. Binding of drugs to biological material. In: Graubart, J.I. (Ed.), Handbook of Basic Pharmacokinetics. , 5th ed. American Pharmaceutical Association, Washington, DC, pp. 119–133.
Sharma, P., Denny, W.A., Garg, S., 2009. Effect of wet milling process on the solid state of indomethacin and simvastatin. Int. J. Pharm. 380, 40–48.
Strickley, R.G., 2004. Solubilizing excipients in oral and injectable formulations. Pharm. Res. 21, 201–230.
Wong, J., Brugger, A., Khare, A., Chaubal, M., Papadopoulos, P., Rabinow, B., Kipp, J., Ning, J., 2008. Suspensions for intravenous (IV) injection: a review of development, preclinical and clinical aspects. Adv. Drug Deliv. Rev. 60, 939–954.
Yang, G., Ran, Y., Yalkowsky, S.H., 2002. Prediction of the aqueous solubility: comparison of the general solubility equation and the method using an Amended solvation energy relationship. J. Pharm. Sci. 91, 517–533.
Zhang, G.G., Gu, C., Zell, M.T., Burkhardt, R.T., Munson, E.J., Grant, D.J., 2002. Crystallization and transitions of sulfamerazine polymorphs. J. Pharm. Sci. 91, 1089–1100.